

**Atom nanolithography with multilayer light masks: Particle optics analysis**R. Arun,<sup>1</sup> I. Sh. Averbukh,<sup>1</sup> and T. Pfau<sup>2</sup><sup>1</sup>*Department of Chemical Physics, The Weizmann Institute of Science, Rehovot, Israel*<sup>2</sup>*5th Institute of Physics, University of Stuttgart, Germany*

(Received 20 March 2005; published 25 August 2005)

We studied the focusing of atoms by multiple layers of standing light waves in the context of atom lithography. In particular, atomic localization by a double-layer light mask is examined using the optimal squeezing approach. Operation of the focusing setup is analyzed both in the paraxial approximation and in the regime of nonlinear spatial squeezing for the thin-thin, as well as thin-thick, atom lens combinations. It is shown that the optimized double light mask may considerably reduce the imaging problems, improve the quality of focusing, and enhance the contrast ratio of the deposited structures.

DOI: [10.1103/PhysRevA.72.023417](https://doi.org/10.1103/PhysRevA.72.023417)

PACS number(s): 32.80.Lg, 03.75.Be, 42.82.Cr, 03.65.Sq

**I. INTRODUCTION**

Since the early demonstration of submicron atom lithography [1], the subject of focusing neutral atoms by use of light fields continues to attract a great deal of attention. The basic principle of atom lithography relies on the possibility of concentrating the atomic flux in space, by utilizing spatially modulated atom-light interactions. In the conventional atom-lithographic schemes, a standing wave (SW) of light is used as a mask on atoms to concentrate the atomic flux periodically and create desired patterns at the nanometer scale [2]. The technique has been applied to many atomic species in one- [3–11] as well as two-dimensional [12] pattern formations. There are two ways to focus a parallel beam of atoms by light masks in close correspondence with conventional optics. In the thin-lens approach, atoms are focused outside the region of the light field which happens for low-intensity light beams. On the other hand, the atoms can be focused within the light beam when its intensity is high. This is known as the thick-lens regime and is very similar to the graded-index lens of traditional optics. The laser focusing of atoms depends on parameters such as the thickness of light beams, the velocity spread of atoms, detuning of the laser frequency from the atomic transition frequencies, etc. Experimentally, atomic nanostructures have been reported with sodium [1,5], chromium [6,7], aluminum [8], cesium [9], ytterbium [10], and iron [11] atoms.

Most theoretical studies of atom lithography employ a particle optics approach to laser focusing of atoms [3,4,13]. The classical trajectories of atoms in the light-induced potential suffice to study the focal properties of the light lens. In the case of direct laser-guided atomic deposition, the diffraction resolution limit will be ultimately determined by the de Broglie wavelength of atoms and may reach several picometers for typical atomic beams [14]. In practice, however, this limit has never been relevant because of the surface diffusion process, the quality of the atomic beam, and severe aberrations due to anharmonicity of the sinusoidal dipole potential. As a result, all current atom lithography schemes suffer from a considerable background in the deposited structures. A possible way to overcome the aberration problem was suggested in [15] by using nanofabricated mechanical masks that block atoms passing far from the minima of the

dipole potential. However, this complicates considerably the setup and reduces the deposition rate. Therefore, there is a considerable need for a pure atom optics solution for the enhanced focusing of an atomic beam having a significant angular spread.

In the paraxial approximation, the steady-state propagation of an atomic beam through a standing light wave is closely connected to the problem of the time-dependent lateral motion of atoms subject to a spatially periodic potential of an optical lattice. From this point of view, enhanced focusing of the atomic beam can be considered as a squeezing process on atoms in the optical lattice. In a recent work [16], a squeezing technique has been introduced for atoms in a pulsed optical lattice. This approach considered a time modulation of the SW with a series of short laser pulses. Based on a specially designed aperiodic sequence of pulses, it has been shown that atoms can be squeezed to the minima of the light-induced potential with a reduced background level. Oskay *et al.* [17] have verified this proposal experimentally using Cs atoms in an optical lattice. In Refs. [16,17], the atoms were loaded into the optical lattice and the dynamics of atoms along the direction of the SW was studied as a time-dependent problem. The aim of the present study is to extend the focusing scenario of Ref. [16] to the beam configuration employed for atomic nanofabrication. We generalize the results on atomic squeezing in the pulsed SW to a system involving the atomic beam traversing several layers of light masks. In particular, we will investigate prospects for reducing spherical and chromatic aberrations in atom focusing with double-layer light masks. High-resolution deposition of chromium atoms will be considered as an example.

The structure of this paper is as follows. In Sec. II, the basic framework of the problem is defined and the linear focusing of atoms by a double-layer light mask is studied, using the particle optics approach in the paraxial approximation. In Sec. III, we examine the optimal squeezing scheme of [16] when applied to the atomic-beam traversing two layers of light masks. The effects of beam collimation and chromatic aberrations are considered in Sec. IV. Here, we optimize the double-lens performance and give parameters for the minimum spot size in the atomic deposition. Finally, in Sec. V, we summarize our main results.

## II. FOCUSING OF ATOMS BY MULTILAYER LIGHT MASKS: A CLASSICAL TREATMENT

The focusing property of single-SW light has been studied in great detail by McClelland *et al.* [4,6]. The light acts like an array of cylindrical lenses for the incident atomic beam, focusing the atoms into a grating on the substrate. However, because of the nonparabolic nature of the light-induced potential, the focusing of atoms is subject to spherical aberrations giving a finite width to the deposited features [4]. A pair of light masks, made from two standing light waves, may in principle reduce the focusing imperfections due to a clear physical mechanism. In this configuration, the first SW prefocuses the atoms towards the minima of the sinusoidal potential. When the prefocused atoms cross the second SW, they see closely the parabolic part of the potential which should result in a reduction of the overall spherical aberrations.

To test this scheme, we consider the propagation of an atomic beam through a combination of two SW's formed by counterpropagating laser beams. The two SW's are identical except for their intensities and are assumed to be formed along the  $x$  direction. Atoms are described as two-level systems with transition frequency  $\omega_0$ . We take the direction of propagation of atoms through the SW fields along the  $z$  direction. If the atoms move sufficiently slow (adiabatic conditions) through the light fields, the internal variables of atoms maintain a steady state during propagation [18]. In this approximation, the atoms can be described as pointlike particles moving under the influence of an average dipole force. The potential energy of interaction is given by [13,19]

$$U(x,z) = \frac{\hbar\Delta}{2} \ln[1 + p(x,z)], \quad (1)$$

where

$$p(x,z) = \frac{\gamma^2}{\gamma^2 + 4\Delta^2} \frac{I(x,z)}{I_s}. \quad (2)$$

In Eq. (2),  $\Delta$  is the detuning of the laser frequency from the atomic resonance,  $I(x,z)$  is the light intensity,  $\gamma$  is the spontaneous decay rate of the excited level, and  $I_s$  is the saturation intensity associated with the atomic transition. For the arrangement of two SW light masks (denoted by 1 and 2) with separation  $S$  between them, the net intensity profile of light is given by

$$I(x,z) = \{I_1 \exp(-2z^2/\sigma_z^2) + I_2 \exp[-2(z-S)^2/\sigma_z^2]\} \sin^2(kx). \quad (3)$$

Here,  $\sigma_z$  is the  $1/e^2$  radius and  $\lambda = 2\pi/k$  is the wavelength of laser beams forming the SW's. We consider the Gaussian intensity profiles and ignore any  $y$  dependence of the laser intensities since the force on atoms along the  $y$  direction is negligible compared to that along the SW ( $x$  axis) direction.  $I_1$  and  $I_2$  denote the maximum intensities of the standing light waves 1 and 2, respectively. We neglect the overlap and interference between the two SW's. The intensity profile of light and the focusing of atoms by light fields are shown schematically in Fig. 1.

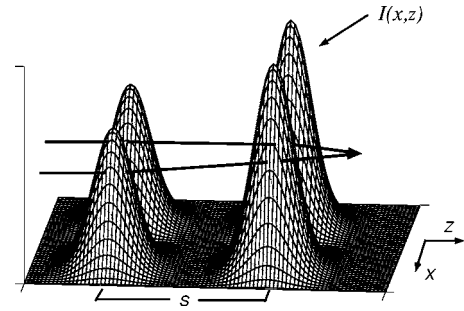


FIG. 1. Schematic representation of laser focusing of atoms by a double layer of Gaussian standing waves. The intensity profile shows the Gaussian envelopes along the  $z$  axis and the sinusoidal variations along the  $x$  axis.

The classical trajectories of atoms in the potential (1) induced by the double-layer light masks obey Newton's equations of motion

$$\frac{d^2x}{dt^2} + \frac{1}{m} \frac{\partial U(x,z)}{\partial x} = 0, \quad \frac{d^2z}{dt^2} + \frac{1}{m} \frac{\partial U(x,z)}{\partial z} = 0. \quad (4)$$

Using the conservation of energy, we can combine the above two equations and solve for  $x$  as a function of  $z$ . This results in two first-order coupled differential equations for  $x(z)$ ,  $\alpha \equiv dx(z)/dz$ :

$$\frac{dx(z)}{dz} = \alpha,$$

$$\frac{d\alpha(z)}{dz} = \frac{1 + \alpha^2}{2(E - U)} \left( \alpha \frac{dU}{dz} - (1 + \alpha^2) \frac{dU}{dx} \right). \quad (5)$$

Here,  $E$  represents the total energy of the incoming atoms (the kinetic energy in the field-free region) and  $\alpha$  gives the slope of the trajectory  $x(z)$ .

We first study the focal properties of the light fields and solve numerically Eq. (5) for an atomic beam that is initially parallel to the  $z$  axis. The linear focal points and principal-plane locations can be obtained by tracing paraxial trajectories as discussed in [4]. Some typical results are shown in Fig. 2, where we present the numerical calculation of a series of atomic trajectories entering the nodal region of both single ( $I_1 \neq 0, I_2 \equiv 0$ ) and double ( $I_1, I_2 \neq 0$ ) light masks. Table I lists the parameters used in the dimensionless units, in which length is expressed in units of  $\lambda$  and frequency is in units  $\omega_r \equiv \hbar k^2/2m$  corresponding to the recoil energy. We have considered the intensities of light SW's to be equal in the case of double light masks. For the other variables, the values close to the experimental parameters of the chromium atom deposition [20] are taken as an example, though the general conclusions to be drawn should apply to other atoms. It can be seen in Fig. 2 that a sharp focal spot appears in the flux of focused atoms [21]. Despite the small size of the focal spot, the overall localization of atoms in the focal plane is not very marked. The atomic background in the focal plane indeed gets reduced with double light masks as shown in the inset of Fig. 2(c); however, this effect is not very pronounced. To take full advantage of the double-mask arrange-

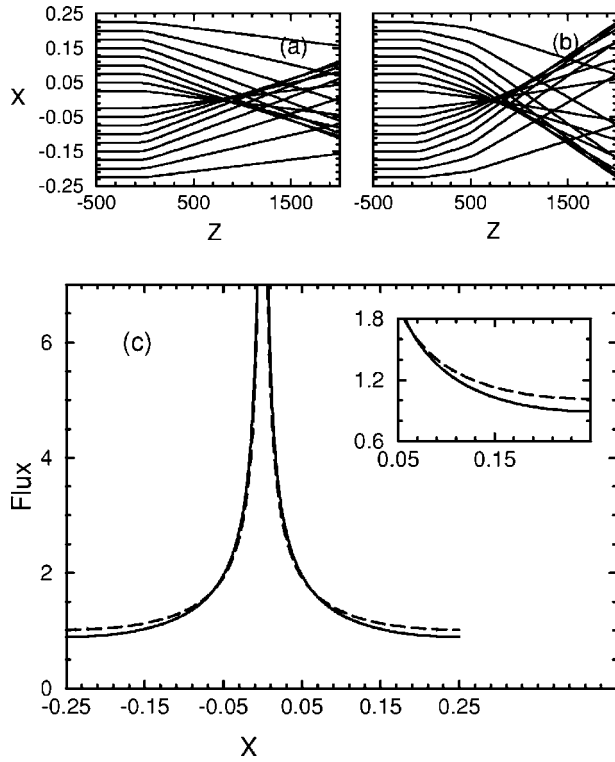


FIG. 2. Numerically calculated trajectories of atoms for laser focusing by a single- (a) and a double- (b) layer light mask. The parameters used are  $I_1/I_s=1000$ ,  $I_2/I_s=0$  (a) and  $I_1/I_s=1000$ ,  $I_2=I_1$ ,  $S=500$  (b). All other parameters are the same as in Table I. The solid (dashed) curve in graph (c) shows the probability density of atoms at the focal point  $z=z_f \approx 650$  (700) of the double (single) light lens. The region to the right of origin ( $x=0$ ) in graph (c) is zoomed and shown in the inset.

ment, we have to replace the concept of linear focusing (useful for paraxial trajectories only) by the notion of optimized nonlinear spatial squeezing.

### III. OPTIMAL SQUEEZING THEORY: APPLICATION TO ATOM NANOLITHOGRAPHY

We have seen that the double light lens leads to some improvement in feature contrast in the focal plane in comparison to the single light lens. However, even for a single SW, the best localization of atoms (maximal spatial compression) is achieved not at the focal plane, but after the linear focusing phenomenon takes place. To characterize the spatial

TABLE I. Parameters in scaled units. Frequency is measured in recoil units and length in units of the optical wavelength. Energy is given in the units of recoil energy  $\hbar\omega_r$ .

Parameter	Numerical value
Spontaneous emission rate $\gamma$	238
Detuning $\Delta$	9500
$1/e^2$ radius of SW $\sigma_z$	120
Energy of the incoming atoms $E$	$3 \times 10^9$

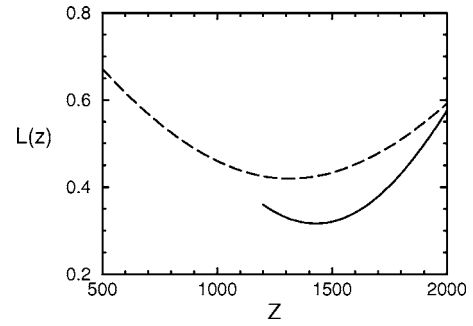


FIG. 3. Localization factor of the atomic distribution for squeezing by a single- (dashed curve) and a double- (solid curve) layer light mask. The parameters used are  $I_1/I_s=1000$ ,  $I_2/I_s=0$  (dashed curve) and  $I_1/I_s=1000$ ,  $I_2=I_1$ ,  $S=S_m \approx 1000$  (solid curve). All other parameters are the same as in Table I. The minimal value of  $L(z)$  is 0.31 (0.42), and it occurs at  $z=z_m \approx 1450$  (1300) for the solid (dashed) curve. In the case of the double light mask, the point  $(z_m, S_m)$  corresponds to the numerically found global minimum of the localization factor.

localization of atoms we use a convenient figure of merit, the localization factor [16]

$$L(z) = 1 - \langle \cos[2kx(z, x_0)] \rangle \equiv \frac{2}{\lambda} \int_{-\lambda/4}^{\lambda/4} dx_0 \{1 - \cos[2kx(z, x_0)]\}, \quad (6)$$

where  $x(z, x_0)$  is the solution of the differential equations (5) satisfying the initial condition  $x \rightarrow x_0$  at  $z \rightarrow -\infty$ . The average in Eq. (6) is taken over the random initial positions of the atoms, and the localization factor is measured as a function of distance  $z$  from the center ( $z=0$ ) of the first SW. The localization factor equals zero for an ideally localized atomic ensemble and is proportional to the mean-square variation of the  $x$  coordinate (modulo standing-wave period) in the case of a well-localized distribution ( $L \ll 1$ ).

Reference [16] considered the squeezing process in the time domain by analyzing the action of pulsed SW's on atoms. In the Raman-Nath approximation, this corresponds to the thin-lens regime (in the space domain) for interaction of a propagating atomic beam with multiple layers of light masks. According to the optimal squeezing strategy [16], the time sequence of pulses applied to the atomic system is determined by minimizing the localization factor. To apply this procedure to atom focusing by the multilayer light masks, we should minimize the localization factor (6) in the parameter space: the separations between the light SW's, their intensities, and the relative distance of substrate surface with respect to the layers of light masks. This optimization can be done numerically using the established simplex-search method. Our numerical analysis shows that the localization factor exhibits multiple local minima even for the simplest case of double light masks. In Fig. 3, we plot the localization factor as a function of distance  $z$  both for single and double light masks around its global minimum  $(z_m, S_m)$ . The intensities of SW's have been chosen to be equal and satisfy the thin-lens condition of atom-light interaction [22]. The graph shows that the localization factor gets a sizable reduction

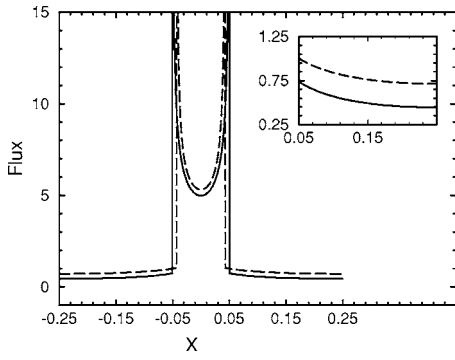


FIG. 4. Probability density of atoms at the point of the best localization by a single- (dashed curve) and a double- (solid curve) layer light mask. The parameters used are  $I_1/I_s=1000$ ,  $I_2/I_s=0$ ,  $z=z_m \approx 1300$  (dashed curve) and  $I_1/I_s=1000$ ,  $I_2=I_1$ ,  $S=S_m \approx 1000$ ,  $z=z_m \approx 1450$  (solid curve). All other parameters are the same as in Table I. The region to the right of origin ( $x=0$ ) is zoomed and shown in the inset.

with double light masks, indicating an enhanced focusing of atoms. The minimum values of  $L(z)$  in Fig. 3 are in conformity with the values obtained for the optimal squeezing of atoms with single and double pulses in the time-dependent problem [16]. We emphasize that the best squeezing (localization) of atoms does not occur at the focal point. Figure 4 displays the spatial distribution of atoms at the point of best localization. Instead of a single focal peak, a two-peaked spatial distribution of atoms near the potential minima is observed in Fig. 4. The origin of these peaks can be related to the formation of rainbows in wave optics and quantum mechanics, and it is discussed in detail in [16,23]. Moreover, on comparing the inset of Figs. 2(c) and 4, it is seen that the optimized separation between the layers of the double light mask results in a considerable reduction of the atomic deposition in the background. This also leads to an overall increased concentration in the atomic flux near the potential minima.

We note that according to [16,17], further squeezing of atoms can be achieved by increasing the number of identical SW's in the multilayer light masks. For the best localization, again the optimized values for the separations between light masks should be used.

In the above analysis, we have considered the case of equal intensities for the light lenses and the problem has been studied in the thin-lens [24] regime of atom focusing by light masks. However, in many current atom-lithographic schemes, focusing of atoms is generally achieved using an intense SW light. This corresponds to the thick-lens regime of the atom-light interaction. In this limit, the focal point is within or close to the region of the laser fields and hence detailed information on the atomic motion within the light is required for a full description [4]. For the chromium atom deposition, the focusing of atoms to the center of an intense SW has been extensively studied both theoretically [4] and experimentally [6]. We show here that a combination of thin and thick lenses can result in the enhanced localization of atoms with minimal background structures. For illustration, we consider the focusing of atoms by a pair of light masks,

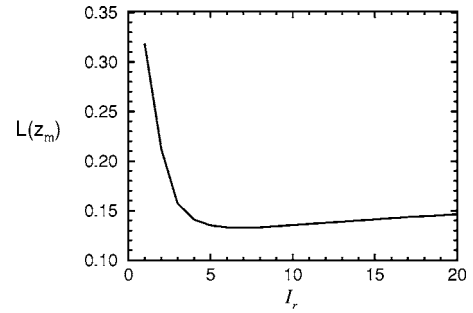


FIG. 5. Minimal localization factor (best atomic localization) of the atomic distribution as a function of the relative intensity  $I_r \equiv I_2/I_1$  of the standing light waves in a double light mask. The parameters used are the same as in Table I with  $I_1/I_s=1500$ .

made of thin and thick lens. We fix the intensity of the first SW light mask to satisfy the thin-lens limit and study the best localization of atoms that can be achieved by varying the intensity of the second SW. A plot of the minimal value of the localization factor versus the relative intensity of the second light mask is shown in Fig. 5. The graph shows that the localization factor becomes almost insensitive to the variation in relative intensity after the intensity ratio reaches the value of 5 and it approaches a small value of  $L=0.15$ . This result is to be compared with the value of  $L=0.31$  for the optimal squeezing by two thin lenses and  $L=0.42$  achievable by a single thin lens. Figure 6 shows the corresponding trajectories of atoms and a plot of the atomic distribution at the point of the best localization. Note that the optimized double light mask reduces the atomic background by a factor of 3 in the midpoint ( $x=0.25$ ) between the two deposition peaks (see the inset of Fig. 6). Moreover, the background in the optimized double mask scheme is 5 times smaller when compared to that of the usual atom deposition in the focal plane (graph not shown) of a single thick lens.

#### IV. PARAMETERS FOR OPTIMAL SQUEEZING OF A THERMAL ATOMIC BEAM

The effects that have been discussed so far assume an initially collimated ( $\alpha=0$ ) beam of atoms with fixed velocity (or energy). However, in atom optics experiments involving thermal atomic beams, the atoms possess a wide range of velocities along the longitudinal ( $z$ -axis) and transverse ( $x$ -axis) directions. In order to characterize the atom focusing under such conditions, we need to average the localization factor, Eq. (6), over the random initial velocities and angles of the beam. The averaging can be done by using the normalized probability density [4]

$$P(v, \alpha) = \frac{1}{2\sqrt{2\pi}} \frac{1}{\alpha_0 v_0^5} v^4 \exp\left[-\frac{v^2}{2v_0^2} \left(1 + \frac{\alpha^2}{\alpha_0^2}\right)\right], \quad (7)$$

where  $v_0$  is the root-mean-square speed of atoms with average energy  $\bar{E} \equiv mv_0^2/2$ . In the above equation, the term proportional to  $v^3 \exp(-v^2/2v_0^2) dv$  represents the thermal flux probability of having a longitudinal velocity  $v$  along the  $z$  direction. The probability of having a transverse velocity

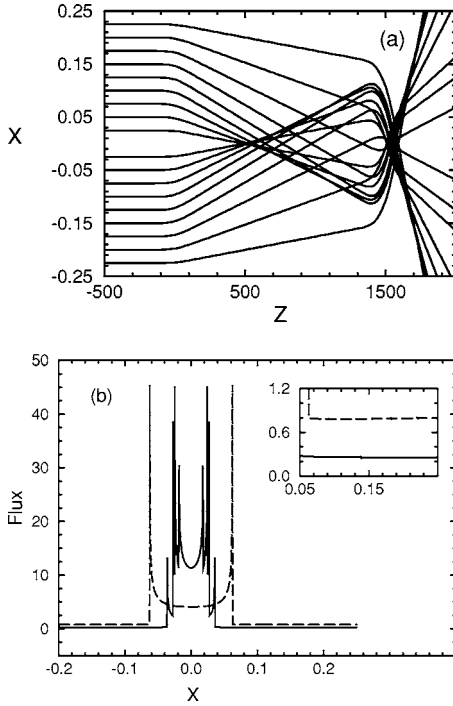


FIG. 6. (a) Numerical trajectory calculation for laser focusing by a double light mask. The parameters used for the calculation are  $I_1/I_s=1500$ ,  $I_2=25I_1$ , and  $S=S_m \approx 1500$ . All other parameters are the same as in Table I. (b) Probability density of the atomic distribution at the point  $(z_m, S_m)$  of maximal squeezing by the double light mask. The parameters used are the same as those of (a) with  $z=z_m \approx 1550$ . The point  $(z_m, S_m)$  is the numerically found global minimum of the function  $L(z)$  with respect to the variables  $(z, S)$ . The dashed curve in graph (b) shows the atomic distribution at the point  $z=z_m$  of the best localization by a single thick light lens with parameters  $I_1/I_s=37500$ ,  $I_2/I_s=0$ ,  $z_m \approx 90$ . The region to the right of origin ( $x=0$ ) is zoomed and shown in the inset.

$v_x = \alpha v$  along the  $x$  direction is proportional to the Gaussian distribution  $\exp(-v_x^2/2v_0^2\alpha^2)dv_x$ , where  $\alpha_0$  is the full width at half maximum (FWHM) of the angular distribution. Using the probability density (7), the averaged localization factor is thus given by

$$L(z) = \frac{2}{\lambda} \int_{\alpha=-\infty}^{\alpha=\infty} \int_{v=0}^{v=\infty} \int_{x_0=-\lambda/4}^{x_0=\lambda/4} P(v, \alpha) \times \{1 - \cos[2kx(z, x_0)]\} dx_0 dv d\alpha. \quad (8)$$

Here,  $x(z, x_0)$  represents the solution of differential equations (5) for varying initial conditions  $(x_0, v, \alpha)$  as  $z \rightarrow -\infty$  of atoms. Note that the solution of Eq. (5) depends on the initial conditions  $(v, \alpha)$  through the energy term  $E \equiv mv^2(1 + \alpha^2)/2$  as well.

Since the focal length of the light mask depends on the velocity of the incoming atoms, the velocity spread in the atomic beam leads to a broadening of the deposited feature size. In the particle optics context of atom focusing, this is referred to as chromatic aberration. In addition, the initial angular divergence ( $\alpha \neq 0$ ) of the atomic beam reduces greatly the focusing of atoms. We are interested in the extent

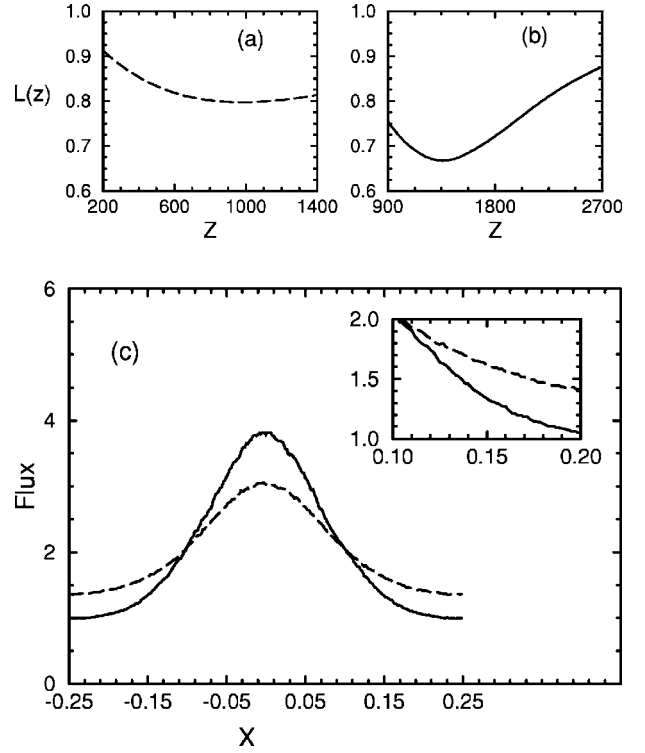


FIG. 7. Localization factor of the atomic distribution for squeezing by a single- (a) and a double- (b) layer light mask. The parameters used are  $\bar{E}=3 \times 10^9$ ,  $\alpha_0=10^{-4}$ ,  $I_1/I_s=1500$ , and (a)  $I_2/I_s=0$ , (b)  $I_2=I_1$ ,  $S=S_m \approx 800$ . All other parameters used are the same as in Table I. The minimal value of  $L(z)$  is 0.67 [0.8], and it occurs at  $z=z_m \approx 1350$  [975] in graph (b) [(a)]. The dashed and solid curves in graph (c) give the atomic distribution at the point  $(z_m, S_m)$  of the best localization by the single- and double-layer light masks with the parameters of (a) and (b). The region to the right of origin ( $x=0$ ) in graph (c) is zoomed and shown in the inset.

to which the velocity and angular spreads degrade the optimal squeezing of atoms. The best feature contrast in the presence of aberrations is again defined by minimizing the localization factor, Eq. (8). We have carried out the triple integration in Eq. (8) numerically and optimized the localization factor  $L(z)$  in the parameter space  $(z, S)$  for the case of double-layer light masks. Figures 7 and 8 display the atomic distribution at the point of the best squeezing by thin-thin and thin-thick lens configurations. On comparing the results with those of a single thin or a thick lens, it is seen that the thin-thick lens combination provides the smallest feature size for the atomic deposition. In the case of thin-thin lenses, the effects of chromatic aberrations are greater because of the strong dependence of focal length on the atomic velocity. We note that, though the initial velocity and angular spread of the thermal beam worsens the optimal squeezing of atoms, the effects may become less important with increasing the number of layers in the multilayer light masks. Furthermore, chromatic aberrations can be greatly reduced by employing low-temperature supersonic beams of highly collimated atoms.

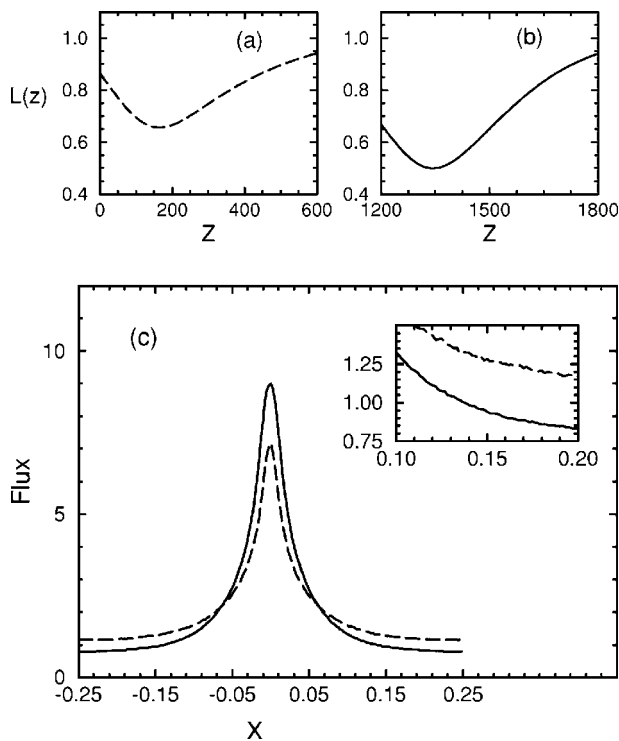


FIG. 8. Localization factor of the atomic distribution for squeezing by a single- (a) and a double- (b) layer light mask. The parameters used are  $\bar{E}=3 \times 10^9$ ,  $\alpha_0=10^{-4}$ , and (a)  $I_1/I_s=37500$ ,  $I_2/I_s=0$ , (b)  $I_1/I_s=1500$ ,  $I_2=25I_1$ ,  $S=S_m \approx 1200$ . All other parameters used are the same as in Table I. The minimal value of  $L(z)$  is 0.5 [0.66] and it occurs at  $z=z_m \approx 1350$  [160] in graph (b) [(a)]. The dashed and solid curves in graph (c) give the atomic distribution at the point  $(z_m, S_m)$  of the best localization by the single- and double-layer light masks with the parameters of (a) and (b). The region to the right of origin ( $x=0$ ) in graph (c) is zoomed and shown in the inset.

## V. SUMMARY

In this paper, we presented particle-optics analysis of atom lithography, using multiple layers of SW light masks. In particular, we studied the spatial focusing of atoms by a double layer of standing light waves with particular reference to minimizing the feature size of atomic deposition. At first, linear focusing of atoms using a paraxial approximation was considered. This showed an improvement in feature contrast at the focal plane, but the effect was rather modest. We then applied the approach of optimal squeezing that was suggested recently for the enhanced localization of atoms in a pulsed SW [16]. We showed that this approach works effectively for atomic nanofabrication and can considerably reduce the background in the atomic deposition. Based on the optimal squeezing approach, a new figure of merit, the localization factor, was introduced to characterize the atomic localization. Both thin-thin and thin-thick lens regimes of atom focusing were considered for monoenergetic as well as thermal beams of atoms. The parameters for the smallest feature size were found by minimizing the localization factor. We have shown that using a proper choice of lens parameters, it is possible to narrow considerably the atomic spatial distribution using a double-layer light mask instead of a single-layer one. Finally, we note that our model calculations neglect the effects of atomic recoil due to spontaneous emissions and dipole force fluctuations. These effects are generally beyond the scope of classical particle optics analysis and can be treated by means of a fully quantum approach. A detailed quantum mechanical study of the optimal atomic squeezing when applied to nanofabrication will be published elsewhere.

## ACKNOWLEDGMENT

This work was supported by the German-Israeli Foundation for Scientific Research and Development.

- 
- [1] G. Timp, R. E. Behringer, D. M. Tennant, J. E. Cunningham, M. Prentiss, and K. K. Berggren, *Phys. Rev. Lett.* **69**, 1636 (1992).
  - [2] For a recent review of atom lithography see M. K. Oberthaler and T. Pfau, *J. Phys.: Condens. Matter* **15**, R233 (2003).
  - [3] K. K. Berggren, M. Prentiss, G. L. Timp, and R. E. Behringer, *J. Opt. Soc. Am. B* **11**, 1166 (1994).
  - [4] J. J. McClelland, *J. Opt. Soc. Am. B* **12**, 1761 (1995).
  - [5] V. Natarajan, R. E. Behringer, and G. Timp, *Phys. Rev. A* **53**, 4381 (1996); R. E. Behringer, V. Natarajan, and G. Timp, *Opt. Lett.* **22**, 114 (1997).
  - [6] J. J. McClelland, R. E. Scholten, E. C. Palm, and R. J. Celotta, *Science* **262**, 877 (1993); W. R. Anderson, C. C. Bradley, J. J. McClelland, and R. J. Celotta, *Phys. Rev. A* **59**, 2476 (1999).
  - [7] U. Drodofsky, J. Stuhler, B. Brezger, T. Schulze, M. Drewsen, T. Pfau, and J. Mlynek, *Microelectron. Eng.* **35**, 285 (1997); Th. Schulze, B. Brezger, P. O. Schmidt, R. Mertens, A. S. Bell, T. Pfau, and J. Mlynek, *ibid.* **46**, 105 (1999); Th. Schulze, T. Müther, D. Jürgens, B. Brezger, M. K. Oberthaler, T. Pfau, and J. Mlynek, *Appl. Phys. Lett.* **78**, 1781 (2001).
  - [8] R. W. McGowan, D. M. Giltner, and S. A. Lee, *Opt. Lett.* **20**, 2535 (1995).
  - [9] F. Lison, H. J. Adams, D. Haubrich, M. Kreis, S. Nowak, and D. Meschede, *Appl. Phys. B: Lasers Opt.* **65**, 419 (1997).
  - [10] R. Ohmukai, S. Urabe, and M. Watanabe, *Appl. Phys. B: Lasers Opt.* **77**, 415 (2003).
  - [11] E. te Slihte, B. Smeets, K. M. R. van der Stam, R. W. Herfst, P. van der Straten, H. C. W. Beijerinck, and K. A. H. van Leeuwen, *Appl. Phys. Lett.* **85**, 4493 (2004); G. Myszkiewicz, J. Hohlfeld, A. J. Toonen, A. F. Van Etteger, O. I. Shklyarevskii, W. L. Meerts, Th. Rasing, and E. Jurdik, *ibid.* **85**, 3842 (2004).
  - [12] R. Gupta, J. J. McClelland, Z. J. Jabour, and R. J. Celotta, *Appl. Phys. Lett.* **67**, 1378 (1995); U. Drodofsky, J. Stuhler, T. Schulze, M. Drewsen, B. Brezger, T. Pfau, and J. Mlynek, *Appl. Phys. B: Lasers Opt.* **65**, 755 (1997).

- [13] J. P. Gordon and A. Ashkin, *Phys. Rev. A* **21**, 1606 (1980).
- [14] A quantum-mechanical analysis of atom lithography has been given by C. J. Lee, *Phys. Rev. A* **61**, 063604 (2000).
- [15] S. Meneghini, V. I. Savichev, K. A. H. van Leeuwen, and W. P. Schleich, *Appl. Phys. B: Lasers Opt.* **70**, 675 (2000).
- [16] M. Leibscher and I. Sh. Averbukh, *Phys. Rev. A* **65**, 053816 (2002).
- [17] W. H. Oskay, D. A. Steck, and M. G. Raizen, *Phys. Rev. Lett.* **89**, 283001 (2002).
- [18] C. Cohen-Tannoudji, J. Dupont-Roc, and G. Grynberg, *Atom-photon Interaction* (Wiley, New York, 1992).
- [19] We assume the dipole force acting on atoms in the light fields to be conservative. For the parameters considered in this paper, the velocity dependence of the light-induced force on atoms can be neglected.
- [20] Dirk Jürgens, Ph.D. dissertation, Universität Konstanz, Germany, 2004.
- [21] In all figures, we normalize the flux such that its integral over the range  $[-\lambda/4, \lambda/4]$  has a value of 1.
- [22] In the thin-lens approximation, the atomic displacement along the standing-wave axis ( $x$  axis) is negligible within the light fields.
- [23] I. Sh. Averbukh and R. Arvieu, *Phys. Rev. Lett.* **87**, 163601 (2001).
- [24] We note that the first experimental demonstration of atom focusing using a thin SW lens was reported by T. Sleator, T. Pfau, V. Balykin and J. Mlynek, *Appl. Phys. B: Photophys. Laser Chem.* **54**, 375 (1992).